



Effect of size and protein environment on electrochemical properties of gold nanoparticles on carbon electrodes

Timur I. Abdullin^{a,*}, Oksana V. Bondar^a, Irina I. Nikitina^a, Emil R. Bulatov^a, Michail V. Morozov^b, Albert Kh. Hilmutdinov^b, Myakzyum Kh. Salakhov^b, Mustafa Çulha^c

^a Faculty of Biology and Soil Science, Kazan State University, Kazan 420008, Tatarstan, Russia

^b Faculty of Physics, Kazan State University, Kazan 420008, Tatarstan, Russia

^c Department of Genetics and Bioengineering, Yeditepe University, Istanbul 34755, Turkey

ARTICLE INFO

Article history:

Received 10 February 2009

Received in revised form 1 June 2009

Accepted 3 June 2009

Available online 11 June 2009

Keywords:

Gold nanoparticles

Proteins

Square-wave voltammetry

Carbon nanotubes

Atomic force microscopy

ABSTRACT

We studied the electrochemical properties of gold nanoparticles (GNPs) and their complexes with proteins using square-wave voltammetry. Effect of the nanoparticle size and detection procedure was explored upon the oxidation of GNPs on a glassy carbon electrode (GCE). For pre-characterized GNPs of 13, 35 and 78 nm diameter, the oxidation peak potential was +0.98, +1.03 and +1.06 V vs. Ag/AgCl, respectively. The conjugation of GNPs with four different proteins was verified by UV-Vis spectroscopy and atomic force microscopy indicated the formation of protein shells around GNPs. This process hampered the oxidation of GNPs on bare GCE causing pronounced decrease in the current response by an average factor of 72. GCE modification with carbon nanotubes weakly influenced the sensitivity of GNP detection but resulted in a 14.5-fold signal increase averaged for all GNP–protein complexes. The acidic dissolution and electrodeposition of GNPs or their complexes adsorbed on GCE allowed superior signal amplification directly proportional to nanoparticle size. The results are useful for the optimization of voltammetric analysis of GNP–protein complexes and can be extended to the characterization of other metal nanostructures and their complexes with biological components.

© 2009 Elsevier B.V. All rights reserved.

1. Introduction

Gold nanoparticles (GNPs) are key nanomaterials intensively studied in different fields of biology and medicine. Particularly, the electronic and optical properties of GNPs are widely exploited for imaging biological objects using microscopy techniques [1,2]. There is a growing interest in biomedical applications of non-spherical gold nanostructures, such as nanorods and nanoshells, which exhibit altered extinction and scattering parameters [2] and cellular uptake mechanism [3] compared to spherical GNPs. Such nanostructures are promising both for the visualization of living cells in vitro and in vivo and their directed damage by means of hyperthermia [4].

The development of biological sensors is another important application of GNPs. In particular, GNPs are used as optical [5–8] and electrochemical [9–12] probes for detecting biomolecules and amplifying biosensor signal. Generally, GNPs improve the analytical performance of biosensor methods by increasing their sensitivity, selectivity and flexibility. To date, different GNP-based biosensors for the analysis of immune components [5,7,8,11,12] and nucleic acids [6,9,10] have been proposed. There are optical biosensors for real-time detection of biomolecule interactions accompanied with a change of

localized plasmon resonance spectra of GNPs in the solution or on the transducer surface [7,8]. The susceptibility of GNPs to non-specific adsorption of biological components decreases the selectivity of such biosensors complicating their practical applications [5]. Electrochemical properties of GNPs can be exploited to develop more selective biosensors for the determination of diagnostic targets [11,12]. The oxidation of GNPs and reduction of gold ions are commonly performed in electrochemical biosensors to produce appropriate analytical signal [9–12].

The above applications of GNPs generally assume their conjugation with biospecific proteins such as antibodies, streptavidin, and protein A to ensure the specificity of developed probes. The conjugation strongly influences the structural and physicochemical properties of GNPs and therefore the performance of GNP–protein complexes as biosensor probes. The dependence of light-absorptive and scattering parameters of GNPs on protein dielectric environments, studied in detail earlier [2,8,13,14], is commonly exploited in biosensor applications [8] as well as for the verification of GNP–protein complexes used in biomedical research [1]. There is a lack of similar studies concerning the effects of protein nanoenvironment on the electrochemical performance of GNPs.

Here, we present the comparative study of voltammetric properties of GNPs and their complexes with several proteins on glassy carbon and carbon nanotube-modified electrodes. The main objective

* Corresponding author. Fax: +7 843 2387121.

E-mail address: tabdulli@gmail.com (T.I. Abdullin).

is to establish the effect of GNPs' size and environment on their electrochemical oxidation in order to increase the sensitivity of their detection. The results obtained can be used for the characterization of GNP–protein biospecific probes and optimization of their analysis using electrochemical biosensors.

2. Experimental

2.1. Reagents and materials

Bovine serum albumin, protein A, avidin, rabbit immunoglobulins G, and multi-walled carbon nanotubes 3–10 nm in diameter and 0.1–10 μm in length were obtained from Sigma-Aldrich. Chloroauric acid ($\text{HAuCl}_4 \times 3\text{H}_2\text{O}$) was purchased from Fluka. To prepare all solutions, deionized water (Milli-Q Element, Millipore) and salts of analytical grade were used.

2.2. Synthesis and modification of gold nanoparticles

Spherical GNPs were synthesized by standard sodium citrate reduction [13]. According to the procedure, sodium citrate was added to the boiling solution of 0.25×10^{-3} M HAuCl_4 under vigorous stirring. After 10 min the resultant solution became stable reddish-purple indicating the completion of nanoparticle synthesis. Citrate concentration in the reaction was adjusted to 1.0, 0.45 and 0.24×10^{-3} M in order to synthesize GNPs of 13, 35 and 78 nm size, respectively [13]. Optical absorption spectra of GNPs were registered on double-beam UV–Vis spectrophotometer Lambda 35 (PerkinElmer). The concentration of GNPs in a suspension estimated by the extinction coefficients [14] varied within 1.4×10^{-11} – 4.8×10^{-9} M depending on the nanoparticle size.

To prepare complexes of GNPs with proteins, the suspension of GNPs was mixed with different amounts of albumin, protein A, avidin or immunoglobulins. Buffers of pH 0.5 units above the isoelectric point of the protein were used to prevent GNP aggregation due to their electrostatic interactions with proteins. The resulted mixture was incubated for 30 min at room temperature allowing protein molecules to bind to the surface of nanoparticle by means of weak interactions. The binding is accompanied with a change of the extinction spectra of GNPs and also stabilizes GNPs against salt aggregation [13]. The latter process can be detected visually by the change of sol colour from purple to grey. We ascertained minimal protein concentrations required for the formation of GNP–protein complexes which prevented the aggregation of GNPs in 0.1 M NaCl. The concentrations ($\mu\text{g mL}^{-1}$) were: 5 for albumin, 3.5 for protein A, and 10 for avidin and immunoglobulins. Prepared complexes containing minimal amount of unbound proteins were analyzed without separation.

2.3. Atomic force microscopy

The size and structure of GNPs and their complexes with proteins were analysed by atomic force microscope NTEGRA Prima (NT-MDT). The scanner (50 μm) equipped with capacitive sensors and silicon cantilevers (curvature 10 nm, spring constant 0.4–2.7 N/m, NT-MDT) were used for scanning. An aliquot of the suspension of GNPs or GNP–protein complex was evenly spread on the surface of freshly-cleaved mica and dried. The samples were analysed in air using the tapping mode with a resonance frequency of 80 kHz, scan rate of 1 Hz and resolution of 256×256 pixels. The tip loading force was minimized to reduce deformation of the sample.

2.4. Electrochemical measurements

Before electrode modification, carbon nanotubes (CNTs) were pre-oxidized in a mixture of nitric and sulphuric acids (1:3, v/v) under ultrasonic agitation. Oxidized water-soluble CNTs were precipitated

by centrifugation, then washed and suspended in deionized water to obtain CNTs concentration of 200 $\mu\text{g/mL}$. An aliquot of CNTs suspension (2 μl) was cast onto the working surface of polished disk glassy carbon electrode (GCE) 1.5 mm in diameter (geometric area 1.8 mm^2) followed by the solvent evaporation. The procedure resulted in modified electrodes characterized by uniform and reproducible surface and good electrochemical performance [15,16].

The common three-electrode cell consisted of bare or modified GCE (working electrode), silver-silver chloride (Ag/AgCl) reference electrode and nickel plate as a counter electrode. Measurements were performed on Autolab PGSTAT12 potentiostat (EcoChemie) using square-wave voltammetry (SWV) or stripping SWV techniques in the potential range from +0.5 to +1.3 V. GPES 4.9 software (EcoChemie) was used for the raw data treatment.

To adsorb nanoparticles on the electrode, an aliquot of GNPs or GNP–protein complex equivalent to 8.6×10^{-15} mol was placed on the working surface of bare GCE or carbon nanotube-modified GCE, dried in laminar air flow followed by the registration of anodic voltammograms of adsorbed nanoparticles in the absence of redox species from the supporting electrolyte (0.01 M sodium acetate in 0.1 M NaCl, pH 5.0). This procedure allows stable attachment of GNPs to the electrode to obtain reproducible voltammograms.

Under stripping conditions, the electrode modified with GNPs was immersed in a mixture of 0.1 M solutions of hydrochloric and nitric acids which dissolved gold nanoparticles to gold ions. Concurrently with dissolution, the reduction of gold ions was performed at the potential of -0.8 V to re-deposit metallic gold on the electrode. After deposition step, the potential scanning was applied to determine the accumulated gold. The optimal time for the electrodeposition of GNPs under experimental conditions was 10 min; further increase of this step duration did not result in the signal amplification. All presented values of SWV current were the mean \pm S.D. of at least three measurements. Registered changes of analytical signal were statistically relevant ($P \leq 0.05$).

3. Results

3.1. Electrochemical properties of gold nanoparticles of different size

Fig. 1 shows visible absorbance spectra of synthesized spherical GNPs with a characteristic plasmon peak arose from the light absorption by electron cloud of the nanoparticles. Upon a decrease of the concentration of reductant used for GNP synthesis their peak

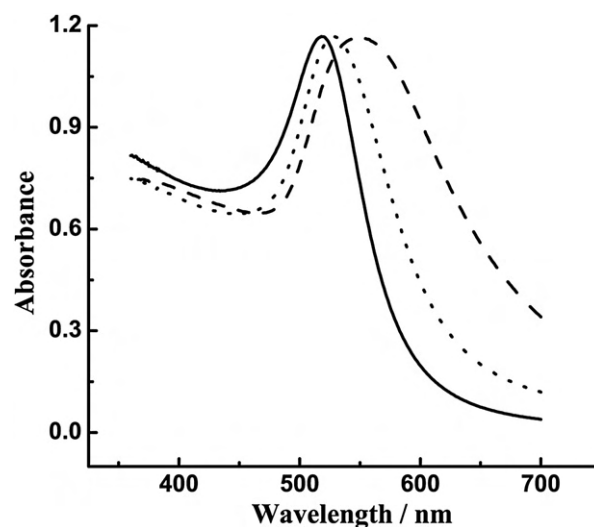


Fig. 1. Optical absorbance spectra of spherical gold nanoparticles of different size synthesized by sodium citrate reduction. The curves with λ_{max} of 518 (solid), 529 (dots) and 550 (dash) nm correspond to the nanoparticles of 13, 35 and 78 nm, respectively.

wavelength (λ_{\max}) shifted towards the red region due to an increase of the nanoparticle size [2,13]. Three synthesized GNP samples exhibited λ_{\max} of 518, 529 and 550 nm. According to reported relationship [13], the average diameter of the nanoparticles calculated from their λ_{\max} value was 13, 35 and 78 nm, respectively.

Atomic force microscopy (AFM) data confirmed that the optical spectra of GNPs are generally in accordance with their real size. As an example, Fig. 2(a) represents AFM image of the smallest GNPs (λ_{\max} 518 nm) on mica substrate where one can observe individual spherical nanoparticles and their aggregates. The average diameter of these GNPs measured by height was 14 ± 3 nm (Fig. 2(d)).

Fig. 3 represents the anodic square-wave voltammograms of GNPs adsorbed on bare GCE. A clear peak appears in the voltammogram at a potential of about +1 V vs. Ag/AgCl which corresponds to the

oxidation of metallic gold to Au^{3+} ion. Synthesized GNP samples were found to exhibit different peak potentials which increased gradually along with an increase of λ_{\max} of nanoparticles. Under scanning conditions the potentials for GNPs of λ_{\max} 518, 529 and 550 nm were equal to +0.98, +1.03 and +1.06 V, respectively (Fig. 3).

The oxidation peak potentials of GNPs of different size on GCE modified with carbon nanotubes (CNTs) were similar to those observed on bare GCE. However, there was a difference in the current response of GNPs on the electrodes. Particularly, on bare GCE repetitive potential scanning was accompanied with gradual decrease of the peak height of GNPs as if the nanoparticles were partially oxidized on the electrode. On CNT-modified GCE the oxidation peak of GNPs clearly observed at the first scan disappeared at subsequent scans. This indicates that electrode modification with CNTs leads to

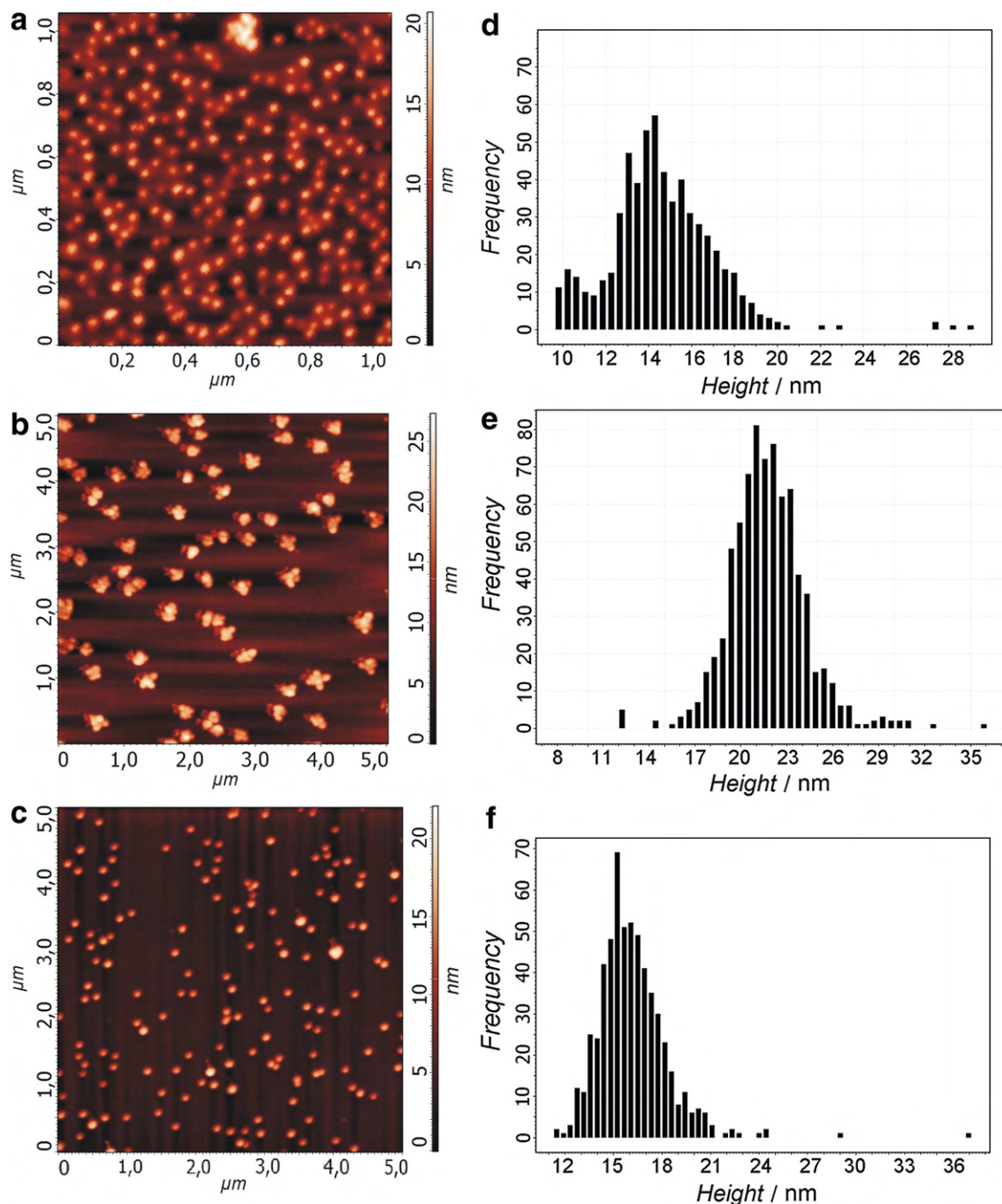


Fig. 2. Topographic AFM images of gold nanoparticles λ_{\max} 518 nm (a), gold nanoparticle–albumin (b) and gold nanoparticle–protein A complexes (c) on mica substrate; d, e, f – corresponding histograms of nanoparticle size distribution.

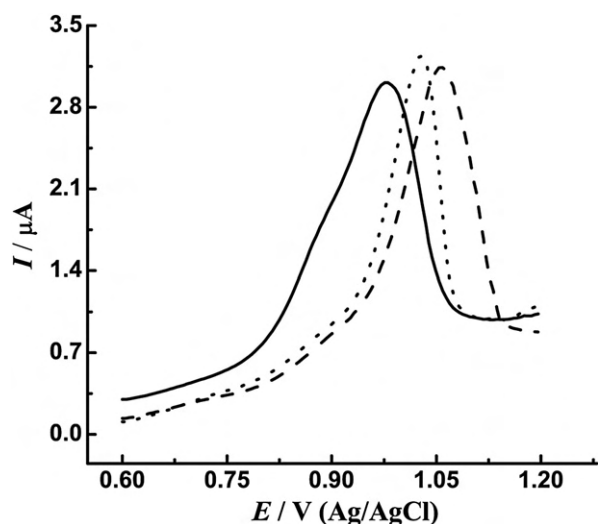


Fig. 3. Square-wave voltammograms of gold nanoparticles on glassy carbon electrode. From left to right the curves correspond to GNPs of 13 (solid), 35 (dots) and 78 (dash) nm, respectively. Scanning parameters: frequency 10 Hz, amplitude 10 mV, step potential 5 mV.

exhaustive oxidation of GNPs at the first scan. In spite of this fact, the current response of GNPs deposited onto bare GCE was higher than that observed on CNT-modified GCE loaded with 3×10^{-15} – 18×10^{-15} mol of GNPs (see [Supplementary information](#)).

This seems to be unexpected because advanced nanostructure and electrocatalytic properties of CNTs considerably promote electrode reactions of various redox species [15–18]. Dissimilar effect in the case of GNPs can be explained by electrostatic repulsion of citrate-capped GNPs from pre-oxidized CNTs, both bearing negatively charged groups on their surface. Another possible reason is that CNTs substantially increase background current on modified GCE at the potentials of around +1 V (due to discharge of electrolyte ions), thereby reducing the sensitivity of GNP detection. For both electrodes used the detection limit of adsorbed GNPs was 0.3×10^{-15} mol that assumes their sensitive determination on carbon electrodes.

In order to further increase the sensitivity of GNP analysis, stripping SWV was applied because of its wide use for the detection of trace amounts of metals [19]. For this purpose, GNPs pre-adsorbed on GCE were subjected to acidic dissolution as described in [Experimental](#). Generated Au^{3+} ions were reduced under controlled potential to re-deposit GNPs on the electrode surface followed by measuring the oxidation current of the deposit. It was found that stripping detection allowed amplification of SWV signal by a factor of 2.6, 3.2 and 5.7 for GNPs of λ_{max} 518, 529 and 550 nm, respectively ([Fig. 4](#)). This shows that under stripping conditions, voltammetric signal of GNPs increases in direct proportion to their size.

3.2. Characterization of gold nanoparticle–protein complexes

For preparation of GNP–protein complexes we utilized the smallest GNPs of λ_{max} 518 nm and several proteins commonly used in biosensor technology, such as albumin, protein A, avidin, and immunoglobulins [20]. The binding of the proteins to GNPs is accompanied with a red-shift of absorption maximum of GNPs by 3–12 nm depending on protein. According to accepted data, the wavelength shift of GNPs is due to the suppression of free electron oscillations of nanoparticle by protein environment [2,13].

Further evidence of the complex formation between GNPs and proteins was obtained with the aid of AFM. As an example, [Fig. 2](#) shows typical AFM images of GNP–albumin and GNP–protein A complexes. The former complex ([Fig. 2\(b\)](#) and (e)) represents well-discernible aggregates of several nanoparticles 22 ± 2 nm in height

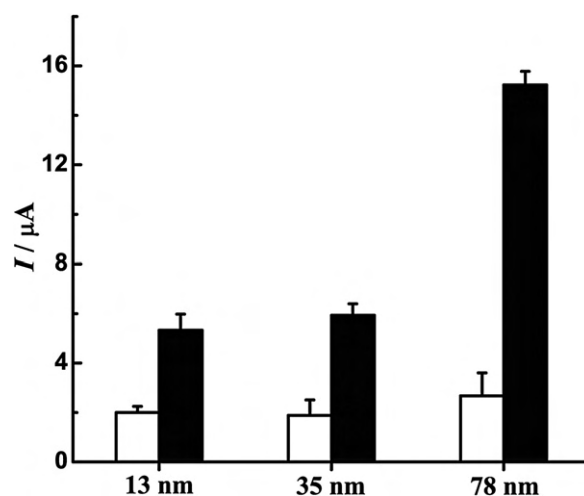


Fig. 4. Oxidation current of gold nanoparticles of different size on glassy carbon electrode registered using direct SWV (white bars) and stripping SWV (dark bars).

which are almost 1.6 times larger than unmodified GNPs. Binding of protein A to nanoparticles on the contrary seems to prevent the aggregation of GNPs. Resulting GNP–protein A complexes are separate spherical nanoparticles 17 ± 3 nm in height. Therefore, according to AFM data, their size is 1.2 times larger than that of unbound GNPs evidently due to the protein shell formation around the nanoparticles ([Fig. 2\(c\)](#) and (f)).

[Table 1](#) summarizes comparative results on voltammetric properties of GNPs and their complexes with proteins on bare GCE and CNT-modified GCE. We ascertained that the conjugation of proteins to GNPs resulted in pronounced decrease in nanoparticle oxidation current on GCE by an average factor of 72 for all proteins. Under the same conditions, but on CNT-modified electrode, GNP–protein complexes produce the current only 10 times lower than GNPs alone ([Table 1](#)).

Although proteins alone were found to exhibit relatively high electrochemical activity on CNT-modified electrode, they were detected at lower overpotentials and at higher concentrations than those used in the experiment. This implies that the proteins did not contribute to the electrochemical oxidation of GNPs. Therefore, the signal amplification observed on CNT-modified GCE is owing to the promotion of oxidation of GNP–protein complexes in the presence of CNTs. Thus, the results showed that direct voltammetric detection of GNPs on carbon electrodes is considerably hindered by the proteins to form insulating shells around the nanoparticles. The use of CNTs reduces this hindering effect evidently due to the ability of CNTs to penetrate into the protein shell and thereby increase the contact of nanoparticle core with electrode surface.

Stripping SWV of GNP–protein complexes was also performed in order to evaluate their voltammetric response after dissolution-

Table 1
Oxidation current (I) and peak potential (E) of gold nanoparticles (λ_{max} 518 nm) and their complexes with proteins on bare GCE and carbon nanotube-modified GCE.

Sample	GCE**		CNT-modified GCE**		Stripping current (nA)***
	I (nA)	E (mV)	I (nA)	E (mV)	
GNPs*	2010 ± 250	+975	1950 ± 100	+964	5330 ± 645
GNP–albumin	37 ± 6	+713	254 ± 53	+730	973 ± 41
GNP–protein A	32 ± 8	+695	182 ± 107	+728	1906 ± 306
GNP–immunoglobulin	6 ± 3	+709	255 ± 53	+720	476 ± 45
GNP–avidin	37 ± 38	+710	109 ± 48	+738	1480 ± 541

* 8.6×10^{-15} mol of GNPs were placed on the electrode.

**Measurements were performed using direct SWV.

***Stripping SWV was performed on bare GCE.

deposition step. We found that anodic stripping current of the complexes on bare GCE was 26–79 times higher than the signal observed upon their direct SWV detection (without pre-stripping stage). Stripping signal of conjugated GNPs approached one for the direct SWV of unbound GNPs but was about 4 times lower than stripping signal of these nanoparticles (Table 1). This demonstrates that stripping analysis substantially improves the sensitivity of GNP–protein complex detection. However, even upon stripping SWV conjugated GNPs did not undergo total oxidation on GCE probably due to a portion of GNPs remained irreversibly bound to the proteins.

4. Discussion

In order to characterize GNPs and their complexes with proteins, SWV was chosen among other voltammetric techniques because it combines high sensitivity, resolution and speed [19]. Cyclic voltammetry was not suitable for the detection of GNPs at concentrations used because of its low sensitivity. We optimized the conditions of GNP detection using SWV to obtain well-defined anodic curves corresponding to the oxidation of gold (Fig. 3).

It was ascertained that voltammetric properties of GNPs depend on their size and detection procedure. Particularly, with increasing average diameter of GNPs from 13 nm to 35 and 78 nm their oxidation peak potential proportionally shifted more positively by almost 30 mV (Fig. 3) similar to hyperchromic shift of nanoparticle λ_{\max} (Fig. 1). As reported earlier [21], GNPs may produce several redox peaks attributed to different redox states of the nanoparticle that is typical of the species with delocalized redox centres. In our case, a certain shift of the anodic potential of GNPs can be explained by the better contact of smaller nanoparticles with the electrode surface that allows them to be oxidized at lower overpotentials compared to GNPs of larger size. In accordance with this assumption, some voltammograms of GNPs, along with the main anodic peak at +1 V, contained minor peaks at lower potentials of about +0.75 V (data not shown) presumably corresponded to an admixture of smaller-size gold nanostructures generated during GNP synthesis.

An increase of GNP size, on the contrary, seems to hamper electron removal from extended bulk substance of the nanoparticle. This is consistent with stripping SWV data which demonstrated that the additional acidic dissolution and subsequent electrodeposition of GNPs on GCE resulted in several-fold amplification of the current response of GNPs. Furthermore, the larger the GNPs, the more relative amplification of the signal (Fig. 4). This implies that pre-stripping stage diminishes steric effect on GNP oxidation due to redistribution of nanoparticle substance on the electrode contributed to an increase of effective surface concentration of GNPs.

The results show the principle possibility of GNP size estimation by measuring their square-wave peak potential (Fig. 3) similarly to spectrophotometric determination of λ_{\max} (Fig. 1) [2,13]. For amplification of the electrochemical signal of GNPs one can use nanoparticles of larger size in combination with their stripping detection because such GNPs appear to be more effective biosensor probes. However, the possible decrease of stability and mass transfer of colloids of increased size must be taken into account.

UV–Vis spectroscopy and AFM were used to verify the attachment of proteins to GNPs. Specifically, we registered the shift of absorbance peak wavelength of GNPs after their conjugation with proteins due to the change of dielectric environment of GNPs [2,13]. Compared to unbound GNPs, their complexes with protein were stable in sodium chloride solution also indicating protein adsorption on the surface of GNPs. AFM of GNP–protein complexes allowed us to observe the formation of protein shells around GNPs (Fig. 2). Protein modification was found to strongly affect the electrochemical oxidation of GNPs (Table 1).

On bare GCE the oxidation current of protein-conjugated GNPs decreased by an average factor of 72 compared to unbound GNPs.

Furthermore, the inhibiting effect was revealed for protein concentrations 10-fold lower than those used to prepare GNP–protein complexes. No noticeable influence of protein characteristics on GNP oxidation was revealed under experimental conditions indicating generally unspecific effect of protein shells on voltammetric behaviour of the complexes. Nevertheless, drastic decrease of current response of GNPs after protein attachment provides the possibility to probe protein–nanoparticle interactions using electrochemical biosensors.

When CNT-modified GCE was used instead of bare GCE the oxidation current of GNP–protein complexes was only 10-fold lower compared to unbound GNPs. This implies that CNTs partially decrease the inhibiting effect of proteins facilitating the detection of protein-surrounded GNPs. This is in agreement with literature data that clearly demonstrated the ability of CNTs to promote electrochemical reactions of difficult-to-access redox centres such as active sites of oxidoreductases [17,18]. Nevertheless, even in the presence of CNTs the electrooxidation of GNP–protein complexes remains suppressed compared to GNPs free of proteins.

Along with the current response, the proteins also affected anodic potentials of GNPs both on bare and CNT-modified GCE. Prepared GNP–protein complexes were found to be oxidized at lower overpotentials by 226–280 mV on the electrodes than unbound GNPs (Table 1). The decrease in oxidation peak potential indicates that redox state of GNPs is changed in the presence of proteins. We suppose that lowered potential of GNP–protein complexes probably corresponds to some portion of GNPs in immediate contact with protein shell whereas another part of the nanoparticle is unavailable for electrode oxidation.

By means of stripping analysis the most effective detection of GNP–protein complexes was achieved. It was found that the dissolution of pre-adsorbed complexes and subsequent re-deposition of GNPs on the electrode diminished the effect of protein shell on the nanoparticle oxidation resulting in the current response commensurable with that for unbound GNPs (Table 1). The results indicate that stripping analysis provides sensitive and customizable detection of GNPs and their complexes with proteins that can be further improved by optimization of GNPs size and voltammetric conditions.

5. Conclusions

The results obtained in this study show the details of electrochemical properties of GNPs concerning the effect of their size and conjugation with proteins on the oxidation on carbon electrodes. The increase of nanoparticle size results in the increase of oxidation peak potential of GNPs as well as the sensitivity of their detection by means of stripping voltammetry. The effect of protein shells that strongly hampered the direct detection of GNPs can be partially reduced by the modification of an electrode with carbon nanotubes and can be almost abolished by the optimization of stripping analysis of GNPs. Proposed approaches are of interest in biosensor applications and can be extended to explore electrochemical properties of different metallic nanostructures and their complexes with biological components.

Acknowledgements

The study was supported in part by the Russian Federal Agency for Science and Innovations government contract FCP 02.552.12.7008.

Appendix A. Supplementary data

Supplementary data associated with this article can be found, in the online version, at doi:10.1016/j.bioelechem.2009.06.002.

References

- [1] K. Sokolov, M. Follen, J. Aaron, I. Pavlova, A. Malpica, R. Lotan, R. Richards-Kortum, Real-time vital optical imaging of precancer using anti-epidermal growth factor receptor antibodies conjugated to gold nanoparticles, *Cancer Res.* 63 (2003) 1999–2004.
- [2] P.K. Jain, K.S. Lee, I.H. El-Sayed, M.A. El-Sayed, Calculated absorption and scattering properties of gold nanoparticles of different size, shape, and composition: applications in biological imaging and biomedicine, *J. Phys. Chem., B* 110 (2006) 7238–7248.
- [3] B.D. Chithrani, W.C.W. Chan, Elucidating the mechanism of cellular uptake and removal of protein-coated gold nanoparticles of different sizes and shapes, *Nano Lett.* 7 (2007) 1542–1550.
- [4] D. Pissuwan, S.M. Valenzuela, M.B. Cortie, Therapeutic possibilities of plasmonically heated gold nanoparticles, *Trends Biotechnol.* 24 (2006) 62–67.
- [5] P. Englebienne, A.V. Hoonacker, J. Valsamis, Rapid homogeneous immunoassay for human ferritin in the cobas mira using colloidal gold as the reporter reagent, *Clin. Chem.* 46 (2000) 2000–2003.
- [6] R.A. Reynolds, C.A. Mirkin, R.L. Letsinger, Homogeneous, nanoparticle-based quantitative colorimetric detection of oligonucleotides, *J. Am. Chem. Soc.* 122 (2000) 3795–3796.
- [7] N. Nath, A. Chilkoti, A colorimetric gold nanoparticle sensor to interrogate biomolecular interactions in real time on a surface, *Anal. Chem.* 74 (2002) 504–509.
- [8] K. Fujiwara, H. Watarai, H. Itoh, E. Nakahama, N. Ogawa, Measurement of antibody binding to protein immobilized on gold nanoparticles by localized surface plasmon spectroscopy, *Anal. Bioanal. Chem.* 386 (2006) 639–644.
- [9] J. Wang, D. Xu, A.-N. Kawde, R. Polsky, Metal nanoparticle-based electrochemical stripping potentiometric detection of DNA hybridization, *Anal. Chem.* 73 (2001) 5576–5581.
- [10] M. Ozsoz, A. Erdem, D. Ozkan, P. Kara, H. Karadeniz, B. Meric, K. Kerman, S. Girousi, Allele-specific genotyping by using guanine and gold electrochemical oxidation signals, *Bioelectrochemistry* 67 (2005) 199–203.
- [11] Z.-P. Chen, Z.-F. Peng, P. Zhang, X.-F. Jin, J.-H. Jiang, X.-B. Zhang, G.-L. Shen, R.-Q. Yu, A sensitive immunosensor using colloidal gold as electrochemical label, *Talanta* 72 (2007) 1800–1804.
- [12] A. Ambrosi, M.T. Castaneda, A.J. Killard, M.R. Smyth, S. Alegret, A. Merkoci, Double-codified gold nanolabels for enhanced immunoanalysis, *Anal. Chem.* 79 (2007) 5232–5240.
- [13] N.G. Khlebtsov, V.A. Bogatyrev, L.A. Dykman, A.G. Melnikov, Spectral extinction of colloidal gold and its biospecific conjugates, *J. Colloid Interface Sci.* 180 (1996) 436–445.
- [14] X. Liu, M. Atwater, J. Wang, Q. Huo, Extinction coefficient of gold nanoparticles with different sizes and different capping ligands, *Colloids Surf., B* 58 (2007) 3–7.
- [15] T.I. Abdullin, I.I. Nikitina, D.G. Ishmukhametova, G.K. Budnikov, O.A. Konovalova, M.Kh. Salakhov, Carbon nanotube-modified electrodes for electrochemical DNA-sensors, *J. Anal. Chem.* 62 (2007) 599–603.
- [16] T.I. Abdullin, I.I. Nikitina, O.V. Bondar, Detection of DNA depurination with the use of an electrode modified with carbon nanotubes, *J. Anal. Chem.* 63 (2008) 690–692.
- [17] A. Merkoci, M. Pumera, X. Llopis, B. Perez, M. Valle, S. Alegret, New materials for electrochemical sensing VI: carbon nanotubes, *Trends Anal. Chem.* 24 (2005) 826–838.
- [18] D. Ivnitski, K. Artyushkova, Surface characterization and direct electrochemistry of redox copper centers of bilirubin oxidase from fungi *Myrothecium verrucaria*, *Bioelectrochemistry* 74 (2008) 101–110.
- [19] J. Wang, *Analytical Electrochemistry*, 2nd ed. Wiley-VCH, New York, 2000.
- [20] D.S. Wilson, S. Nock, Functional protein microarrays, *Curr. Opin. Chem. Biol.* 6 (2001) 81–85.
- [21] B.M. Quinn, P. Liljeroth, V. Ruiz, T. Laaksonen, K. Kontturi, Electrochemical resolution of 15 oxidation states for monolayer protected gold nanoparticles, *J. Am. Chem. Soc.* 125 (2003) 6644–6645.